Annals of 3D Printed Medicine 2 (2021) 100014

Contents lists available at ScienceDirect

Annals of 3D Printed Medicine

journal homepage: www.elsevier.com

Research paper

3D printed prototype of a complex neuroblastoma for preoperative surgical planning

A. Tejo-Otero[a,*], F. Fenollosa-Artés[a,e], R. Uceda[a,e], A. Castellví-Fernández[a], P. Lustig-Gainza[a], A. Valls-Esteve[b], M. Ayats-Soler[b], J. Munuera[b,d], I. Buj-Corral[e], L. Krauel[b,c]

[a] Centre CIM, Universitat Politècnica de Catalunya (CIM UPC), Carrer de Llorens i Artigas, 12, 08028, Barcelona, Spain
[b] 3D4H Unit, Hospital Sant Joan de Déu, Universitat de Barcelona, Spain
[c] Surgery Department, Hospital Sant Joan de Déu, Universitat de Barcelona, Spain
[d] Diagnostic Imaging Department, Hospital Sant Joan de Déu, Universitat de Barcelona, Spain
[e] Universitat Politècnica de Catalunya, Departament of Mechanical Engineering, School of Engineering of Barcelona (ETSEIB), Av. Diagonal, 647, 08028, Barcelona, Spain

ARTICLE INFO

Article History:
Received 23 April 2021
Revised 26 April 2021
Accepted 26 April 2021
Available online 4 May 2021

Key Words:
3D printing
Surgical planning
Neuroblastoma
Fused filament fabrication
Selective laser sintering
Additive manufacturing

ABSTRACT

Neuroblastoma is the most common abdominal solid tumour in childhood. Its removal implies a complex surgery that requires surgical experience due to the usual encassement of major abdominal blood vessels. Standard surgical planning is based on CT or MRI images. However, in complex cases, normal anatomy is altered and it is difficult to interpret. 3D virtual planning and 3D Printing (3DP) can overcome this difficulties of comprehension. The most common 3DP technology used for this cases is material jetting. Nevertheless, this technology is very expensive and cannot be widely used. Consequently, its use is limited. The present study seeks to introduce the possibility of reducing costs whilst mantaining the quality of the 3D printed protypes. A full-process of a neuroblastoma case using hybrid manufacturing combining some FFF and some SLS 3D printed parts is presented. The two processes are carried out separately and then joined in a final assembly. The cost of the prototype was 347 €, which is significantly lower than a prototype 3D printed by material jetting.

1. Introduction

Neuroblastoma is a tumour derived from primitive cells of the sympathetic nervous system and is the most common abdominal solid tumour in childhood [1]. It is mainly located in the adrenal gland. Other locations include the neck and chest. The International Neuroblastoma Risk Group (INRG) defined a series of imaging features seen at the time of neuroblastoma diagnosis that confer a poorer prognosis. This Image-defined risk factors (IDRF) are the encasement of major blood vessels and the grade of infiltration of surrounding organs and tissues among others [2]. Surgery still remains a very important part of its treatment and the presence of IDRF are related with surgical outcomes [3].

Additive Manufacturing (AM) has been widely used in different fields such as electronics, aerospace, motor vehicles and medicine. 3D printing (3DP) is starting to bloom in this last sector, as it is nowadays used for different applications: tissue engineering [4,5], implants [6,7], or surgical planning [8–10]. AM technologies can be classified into seven different categories according to ISO/ASTM 52,900 Standard [11]: binder jetting, direct energy deposition (DED), material extrusion (includes Fused Filament Fabrication –FFF– and paste/slurry-based extrusion, known as Direct Ink Writing –DIW–), material jetting, powder bed fusion (includes selective laser sintering –SLS– and selective laser melting –SLM–), sheet lamination and vat photopolimerization (includes stereolithography –SLA– and Digital Light Processing –DLP-). Amongst them, vat photopolymerization, material extrusion, powder bed fusion for plastic parts (SLS) and material jetting are the technologies commonly used for surgical planning prototypes.

In recent years, an effort has been made in the manufacture of more realistic 3D models. For example, Krauel and Fenollosa-Artés et al. [12] attempted to 3D print three different neuroblastoma prototypes using material jetting (PolyJet® technology by Stratasys®). This was an important advance back in 2016. However, the mechanical properties of the materials used, TangoBlackPlus™ and VeroWhite™, are still far from soft tissue anatomical viscoelastic and mechanical characteristics. This can be confirmed by Bezek et al. [13], who measured several properties of the TangoBlackPlus™ such as: (1) ultimate tensile strength near 500 kPa and (2) elastic modulus over 200 kPa. Regarding the VeroWhite, its tensile strength is 60–70 MPa and its Young's modulus around 2.5 MPa. The elasticity values

* Corresponding author.
E-mail address: atejo@cimupc.org (A. Tejo-Otero).

https://doi.org/10.1016/j.stlm.2021.100014

mentioned are very different to that of real soft tissue anatomy [14–18], which is lower than 20 kPa. Additionally, Meisel et al. [19] manufactured multi-material structures with different VeroWhite™ and TangoBlackPlus™ compositions and carried out several Dynamic Mechanical Analysis (DMA) tests. The measured values of both storage and loss modulus were very high, in the range of MPa, in comparison to soft tissue viscoelastic properties, which were in the range of 2–20 kPa [20–23].

Therefore, there is still a gap between the mechanical and viscoelastic properties of materials and real soft tissue anatomy, but it is possible to reach higher goals by finding new materials that would be able to mimic the properties of real soft tissue anatomy. Moreover, the costs of most materials – as those above metioned used in material jetting- are very high and need to be reduced in order to extend the use of 3D printed prototypes for surgical planning.

Other AM technologies have different issues. For example, common FFF (Fused Filament Fabrication) based desktop 3D printers, only were able to manufacture mono material and mono color prototypes making it difficult to identify the different anatomical structures within the surgical planning prototype. Despite that, it is a cost-effective technology. Thus, SLS (Selective Laser Sintering) has also been used, but for 3D printing rigid and monomaterial prototypes that were later painted to highlight anatomical structures [12,23]. This 3D printing technique is cheaper than material jetting. Moreover, with these two mentioned technologies, it is possible to manufacture an outer mould, in which translucent and soft silicone or hydrogel is cast. However, this method takes not only a lot of time, but also a lot of effort. The steps of the process are as follows: (1) manufacture of internal structures and outer mould; (2) painting; (3) placing the parts of the outer mould together; (4) silicone or hydrogel casting; and (5) curing and postprocessing.

Therefore, as material jetting is expensive, it limits the spread of AM technologies and its associate benefits for surgical planning. The aim of this study is to show a full-process of a neuroblastoma case using hybrid manufacturing, in other words, combining some FFF and some SLS 3D printed parts. The two processes are carried out separately.

2. Materials and methods

2.1. Image acquisition

Images were acquired with computer tomography (CT), (256 iCT Philips). Fig. 1 depicts the contrast enhanced abdominal portal-phase CT scanner after 3 cycles of induction chemotherapy according to protocol of a 3y old girl with a high risk neuroblastoma with image defined risk factors (IDRF) [24]. Gross total resection (GTR) of the mass, that is, more than 95% of all visible and palpable tumor is recommended for these cases. The surgery is a very demanding one and a thorough surgical planning is adviced. Note the difficulty to differenciate the tumor (red) from the liver (blue) and the relationship with the inferior vena cava and portal veins. The use of 3D virtual reconstructions and 3DP surgical planning prototypes can help the surgical planning of critical aspects of the surgery such as the anatomical location of encased vessels.

Fig. 1. CT scanner of the neuroblastoma case. Red and blue outlines of tumor and liver have been drawn up manually over the DICOM. (For interpretation of the references to color in this figure legend, the reader is referred to the web version of this article.)

2.2. Image segmentation, surface reconstruction, design and 3D printing

The development workflow of the surgical planning prototype can be seen in Fig. 2. The images obtained using CT scan are saved in DICOM (Digital Imaging and Communications in Medicine) format (Fig. 2A). Image segmentation is the process carried out in which several CT Dicom files are overlapped for the 3D virtual reconstruction of the image (Fig. 2B). A semi-automatic segmentation density-based was carried out using IntelliSpace Portal from Philips®.

Image segmentation and 3D virtual reconstructions allow to highlight important aspects of the anatomy in different colors (Fig. 2B): (1) the hepatic artery in red, (2) the tumor in purple, (3) the inferior vena cava in blue, (4) the portal system in green; (5) bone references in white; (6) kidneys in brown; and (7) transparency for the liver.

Two different parts are manufactured separately. The tumor, blood vessels and the kidney were manufactured using polyamide (PA) 12 with the SLS technology (Fig. 2C). The 3D printer used was a Ricoh AM S5500P, which has a layer thickness of 0.08–0.1 mm, at CIM UPC facilities. Once it was 3D printed, the different parts were painted to highlight each anatomical structure. Additionally, in the presented case, the area of the tumor was 3DP leaving circular spots in the tumor wall that allowed to see the inside anatomy that was encased by the tumor such as the superior mesenteric artery and renal vessels.

On the other hand, the liver and portal system was 3D printed on FFF technology (see Fig. 2D) by using a multi-material 3D printer developed at CIM UPC facilities (see Fig. 3). Table 1 summarises the different parameters need to be chosen for the manufacture of the FFF liver part. Each STL has to undergo a pre-processing before 3D printing. Regarding the FFF 3D printing, three materials were used (see Table 2): green and sand colored TPU (Thermoplastic Polyurethane) and PVA (Polyvynil Alcohol). When the 3D printing was finished, the PVA materialising support structures was removed by means of immersion in water.

3. Results

3.1. Surgical planning prototype

Once both parts were 3D printed, they were placed together. Fig. 4, shows the final prototype. Regarding the FFF parts, they were left for 24 h in water in order to remove the PVA support. The 3DP prototype was used for surgical planning prior to surgery as well as for communication purposes with the family for a better understanding of the nature of the condition and the surgery that was needed to be performed. The 3DP prototype was sterilized with low temperature Hydrogen Peroxide (HPO) Sterilizer Matachana 130HPO-2® at a maximum exposition temperature of 54 °C and a program time of 51 min and brought to the Operation Room so it could be checked any time during surgery by the surgical team.

Table 3 summarises the costs in terms of materials and labour.

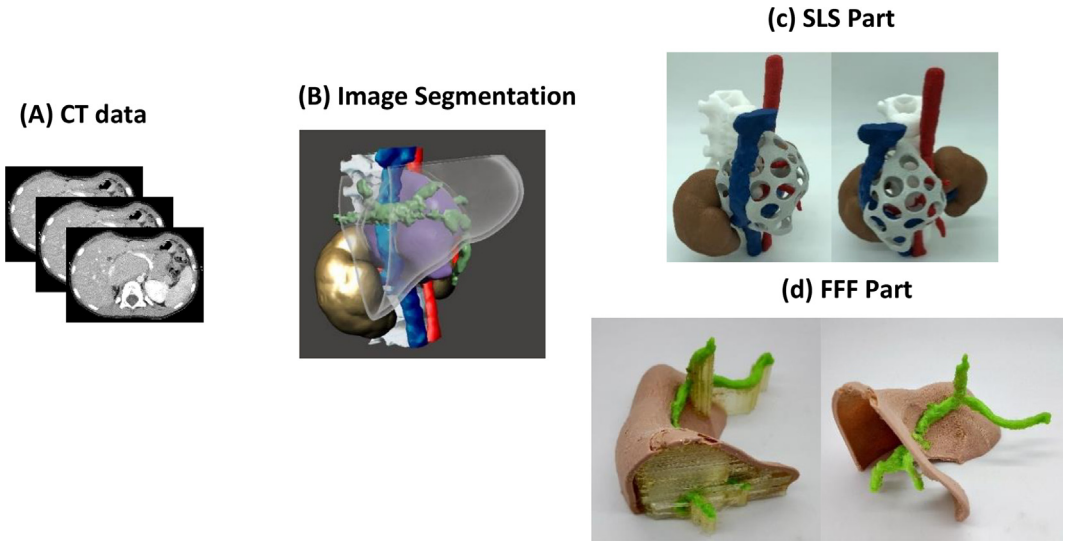

Fig. 2. (A) CT data. (B) Image segmentation. (C) SLS part. (D) FFF part: green part is the biliary tract. (For interpretation of the references to color in this figure legend, the reader is referred to the web version of this article.)

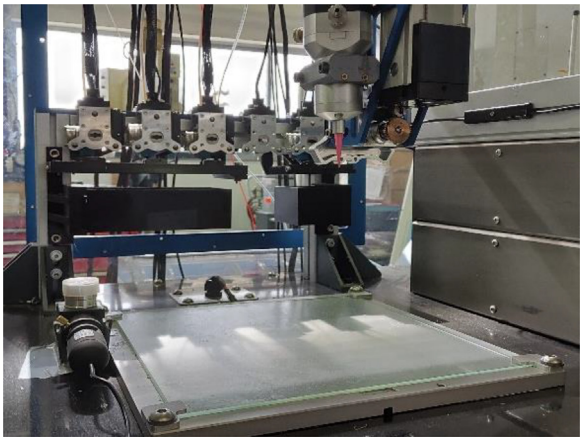

Fig. 3. Multi-material 3D printer.

Table 1
Printing parameters for the 2-process 3D printing of the liver part. T0: corresponds to the first tool of the multi-material 3D printer, which was the sand color TPU filament for the liver .T1: corresponds to the second tool of the multi-material 3D printer, which was the PVA filament for the support. T2: corresponds to the third tool of the multi-material 3D printer, which was the green color TPU filament for the biliary tract.

Process	Parameters	Value
Process 1 (T1/T2)	Layer Height [mm]	0.15
	# Top Solid Layers	8
	# Bottom Solid Layers	5
	# Shells	3
	Infill (FF) [%]	10
	Infill Angle [%]	45/−45
	Printing Speed [mm/s]	2000
Process 2 (T0/T1)	Layer Height [mm]	0.15
	# Top Solid Layers	6
	# Bottom Solid Layers	5
	# Shells	3
	Infill (FF) [%]	8
	Infill Angle [%]	45/−45
	Printing Speed [mm/s]	2600

4. Discussion

The manufacture of multi-material 3DP parts is a promising path that opens the door to the possibility of having prototypes with different materials that have different properties. 3DP phantoms can help achieve better surgical outcomes, especially in oncological surgeries or other conditions were patients have a unique form of presentation or uncommon and distorted anatomical characteristics. Additionally, using different materials, is an initial approach to better simulate the different aspects of real anatomy. It is true that the multi-material prototypes that are manufactured with FFF materials are mostly rigid. Nevertheless, prototypes can be created with different colors highlighting important anatomical structures. Moreover, TPU offers a flexibility as well as more softness than PLA. With this in mind, this novel approach for the manufacture of surgical planning prototypes demonstrates that it is possible to 3D print cost-effective realistic models.

The process in the manufacture of the 3D model took 48 h to complete, less than Witowski et al. [25]. Additionally, its cost was cheaper when compared to material jetting prototypes, and has a price around 2000 € [12].

5. Conclusion

The present study explains the possibility of combining different AM technologies together for the manufacture of 3D printed prototypes. In this paper, a prototype was manufactured using two different technologies such as SLS and FFF. This approach led to a

Table 2
Printing parameters of the FFF materials.

	PVA	TPU
Active/Standby Temperature [°C]	210/170	235/170
Extrusion Width [mm]	0.5	0.5
Nozzle Diameter [mm]	0.4	0.4
Primary Layer Height	0.15	0.15
Retraction Distance [mm]	5.5	10
Extra Restart Distance [mm]	0.1	0.1
Retraction Vertical Lift [mm]	1.5	1.5
Retraction Speed [mm/s]	1000	720

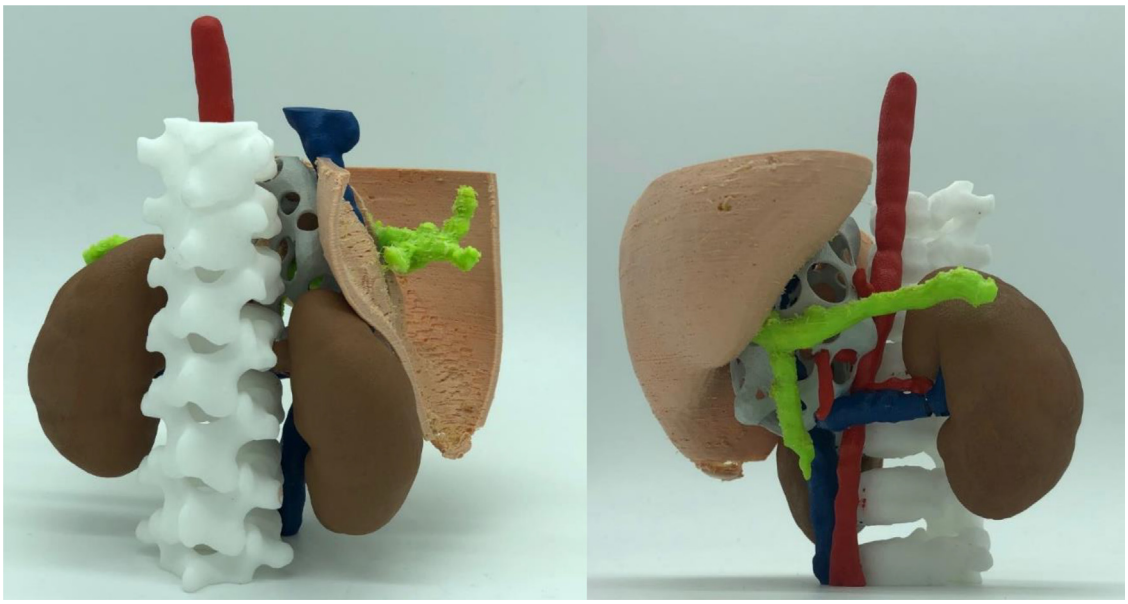

Fig. 4. Surgical planning prototype of a neuroblastoma case with image defined risk factors (IDRF).

Table 3
Cost of the materials for the manufacture of the surgical planning prototype.

Process	Material	Material cost [€]	Labour Cost [€]	Total [€]
FFF	TPU FFF Parts	5	75	90
	PVA FFF Parts	10		
SLS	PA 12 SLS Part	117	140	257
Total [€]		132	215	347

significant reduction of costs. The more the costs of the prototype are cut off, the more number of prototypes will be 3D printed because they will be more cost-effective. On the other hand, these 3DP models can also be used for medical and patient education. Combining the sense of touch with the sense of sight, known as the theory of "touch to learn" has demonstrated to increase and consolidate new learnings specially in surgery [26]. 3D printed models can help to prepare a thorough surgical planning for complex cases as well as help patients and their caregivers understand their condition.

Acknowledgments

The research undertaken in this paper has been partially funded by the project named QuirofAM (Exp. COMRDI16-1-0011) funded by ACCIÓ from the Catalan government and ERDF from EU.

References

[1] Brodeur GM. Neuroblastoma: biological insights into a clinical enigma. Nat Rev Cancer 2003;3:203–16. doi: 10.1038/nrc1014.
[2] Monclair T, Brodeur GM, Ambros PF, Brisse HJ, Cecchetto G, Holmes K, Kaneko M, London WB, Matthay KK, Nuchtern JG, Von Schweinitz D, Simon T, Cohn SL, Pearson ADJ. The international neuroblastoma risk group (INRG) staging system: an INRG task force report. J Clin Oncol 2009;27:298–303. doi: 10.1200/JCO.2008.16.6876.
[3] Langham MR, Lautz TB, Malek MM, Austin M, Rhee DS, Madonna MB, Baertschiger RM, Aldrink JH, Nathan JD, Bruny J, Abdessalam S, Meyers RL, Newman EA, Weil BR, Ehrlich P, Dasgupta R, Polites S, Heaton TE. Update on neuroblastoma. J Pediatr Surg 2018. doi: 10.1016/j.jpedsurg.2018.09.004.
[4] Bose S, Vahabzadeh S, Bandyopadhyay A. Bone tissue engineering using 3D printing. Mater Today 2013;16:496–504. doi: 10.1016/j.mattod.2013.11.017.
[5] Buj-Corral I, Bagheri A, Petit-Rojo O. 3D printing of porous scaffolds with controlled porosity and pore size values. Materials (Basel) 2018;11:1–18. doi: 10.3390/ma11091532.
[6] Liu A, Xue GH, Sun M, Shao HF, Ma CY, Gao Q, Gou ZR, Yan SG, Liu YM, He Y. 3D printing surgical implants at the clinic: a experimental study on anterior cruciate ligament reconstruction. Sci Rep 2016;6:1–13. doi: 10.1038/srep21704.
[7] Buj-Corral I, Domínguez-Fernández A, Durán-Llucià R. Influence of print orientation on surface roughness in fused deposition modeling (FDM) processes. Materials (Basel) 2019;12. doi: 10.3390/ma122333834.
[8] Adams F, Qiu T, Mark A, Fritz B, Kramer L, Schlager D, Wetterauer U, Miernik A, Fischer P. Soft 3D-printed phantom of the human kidney with collecting system. Ann Biomed Eng 2017;45:963–72. doi: 10.1007/s10439-016-1757-5.
[9] Tejo-Otero A, Buj-Corral I, Fenollosa-Artés F. 3D printing in medicine for preoperative surgical planning: a review. Ann Biomed Eng 2020;48:536–55. doi: 10.1007/s10439-019-02411-0.
[10] Muguruza Blanco A, Krauel L, Fenollosa-Artés F. Development of a patients-specific 3D-printed preoperative planning and training tool, with functionalized internal surfaces, for complex oncologic cases. Rapid Prototyp J 2019;25:363–77. doi: 10.1108/RPJ-03-2018-0063.
[11] ASTM I. ASTM52900-15 standard terminology for additive manufacturing—general principles—terminology. West Conshohocken, PA.: ASTM International; 2015 n.d..
[12] Krauel L, Fenollosa F, Riaza L, Pérez M, Tarrado X, Morales A, Gomà J, Mora J. Use of 3D prototypes for complex surgical oncologic cases. World J Surg 2016;40:889–94. doi: 10.1007/s00268-015-3295-y.
[13] Bezek LB, Cauchi MP, De Vita R, Foerst JR, Williams CB. 3D printing tissue-mimicking materials for realistic transseptal puncture models. J Mech Behav Biomed Mater 2020;110:103971. doi: 10.1016/j.jmbbm.2020.103971.
[14] Yeh WC, Jeng YM, Hsu HC, Kuo PL, Li ML, Yang PM, Li PC. Young's modulus measurements of human liver and correlation with pathological findings. IEEE Ultrason Symp Proc Int Symp 2001;2:1233–6.
[15] Arda K, Ciledag N, Aktas E, Aribas BK, Köse K. Quantitative assessment of normal soft-tissue elasticity using shear-wave ultrasound elastography. Am J Roentgenol 2011;197:532–6. doi: 10.2214/AJR.10.5449.
[16] Embry AE, Mohammadi H, Niu X, Liu L, Moe B, Miller-Little WA, Lu CY, Bruggeman LA, McCulloch CA, Janmey PA, Miller RT. Biochemical and cellular determinants of renal glomerular elasticity. PLoS One 2016;11:1–25. doi: 10.1371/journal.pone.0167924.
[17] Falland-Cheung L, Scholze M, Hammer N, Waddell JN, Tong DC, Brunton PA. Elastic behavior of brain simulants in comparison to porcine brain at different loading velocities. J Mech Behav Biomed Mater 2018;77:609–15. doi: 10.1016/j.jmbbm.2017.10.026.
[18] J.J. Van Der Loo, J. Jacot, P.H.M. Bovendeerd, B. 08 45, The Development in Cardiac Stiffness in Embryonic, Neonatal and Adult Mice Evaluated with Atomic Force Microscopy, (2008).
[19] Meisel NA, Dillard DA, Williams CB. Impact of material concentration and distribution on composite parts manufactured via multi-material jetting. Rapid Prototyp J 2018;24:872–9. doi: 10.1108/RPJ-01-2017-0005.
[20] Ramadan S, Paul N, Naguib HE. Standardized static and dynamic evaluation of myocardial tissue properties. Biomed Mater 2017;12:25013. doi: 10.1088/1748-605X/aa57a5.
[21] Mattei G, Tirella A, Gallone G, Ahluwalia A. Viscoelastic characterisation of pig liver in unconfined compression. J Biomech 2014;47:2641–6. doi: 10.1016/j.jbiomech.2014.05.017.
[22] Kiss MZ, Varghese T, Hall TJ. Viscoelastic characterization of in vitro canine tissue. Phys Med Biol 2004;49:4207–18. doi: 10.1088/0031-9155/49/18/002.

[23] Tejo-Otero A, Lustig-Gainza P, Fenollosa-Artés F, Valls A, Krauel L, Buj-Corral I. 3D printed soft surgical planning prototype for a biliary tract rhabdomyosarcoma. J Mech Behav Biomed Mater 2020;109:1–11. doi: 10.1016/j.jmbbm.2020.103844.
[24] Monclair T, Brodeur GM, Ambros PF, Brisse HJ, Cecchetto G, Holmes K, Kaneko M, London WB, Matthay KK, Nuchtern JG, von Schweinitz D, Simon T, Cohn SL, Pearson ADJ. INRG task force, the international neuroblastoma risk group (INRG) staging system: an INRG task force report. J Clin Oncol 2009;27:298–303. doi: 10.1200/JCO.2008.16.6876.
[25] Witowski JS, Pędziwiatr M, Major P, Budzyński A. Cost-effective, personalized, 3D-printed liver model for preoperative planning before laparoscopic liver hemihepatectomy for colorectal cancer metastases. Int J Comput Assist Radiol Surg 2017;12:2047–54. doi: 10.1007/s11548-017-1527-3.
[26] Matsumoto JS, Morris JM, Foley TA, Williamson EE, Leng S, McGee KP, Kuhlmann JL, Nesberg LE, Vrtiska TJ. Three-dimensional physical modeling: applications and experience at mayo clinic. Radiographics 2015;35:1965–88. doi: 10.1148/rg.2015140260.